



Received: 05.07.2020

Accepted: 18.10.2020

Published: 22.11.2020

**Citation:** Priya R, Kumar RS, Naiklal SK, Kumar A. (2020). FLOOD INUNDATION MODELLING FOR TUNGABHADRA BASIN USING HEC-RAS: A CASE STUDY OF HARALAHALLI DISCHARGE SITE. *Geographical Analysis*. 9(2): 33-41. <https://doi.org/10.53989/bu.ga.v9i2.8>

**Funding:** None

**Competing Interests:** None

**Copyright:** © 2020 Priya et al. This is an open access article distributed under the terms of the [Creative Commons Attribution License](https://creativecommons.org/licenses/by/4.0/), which permits unrestricted use, distribution, and reproduction in any medium, provided the original author and source are credited.

Published By Bangalore University, Bengaluru, Karnataka

ISSN

Print: 2319-5371

Electronic: XXXX-XXXX

## FLOOD INUNDATION MODELLING FOR TUNGABHADRA BASIN USING HEC-RAS: A CASE STUDY OF HARALAHALLI DISCHARGE SITE

Rashmi Priya<sup>1</sup>, R Shiva Kumar<sup>2</sup>, Shiv Kumar Naiklal<sup>3</sup>, Anjan Kumar<sup>4</sup>

<sup>1</sup> Student, Department of Geography and Geoinformatics, Bangalore University, Bengaluru

<sup>2</sup> Guest Faculty, Department of Geography, Bangalore University, Bengaluru

<sup>3</sup> Scientist, Karnataka State Natural Disaster Monitoring Centre, Bengaluru

<sup>4</sup> Karnataka State Natural Disaster Monitoring Centre, Bengaluru

### Abstract

*The Hydrologic Engineering Center's River Analysis System (HEC-RAS) can model flood events and produce water surface profiles over the length of the modeled stream. Flood Inundation Modelling is important for engineers, planners, and government agencies used for municipal and urban growth planning, emergency action plans, flood insurance rates, and ecological studies. This paper describes the application of the HEC-RAS model for the development of floodplain maps for the part of Tungabhadra River, Haralahalli discharge site that lies in Haveri district of Karnataka. Since most of the flood plain area/area vulnerable to flooding is currently used for agriculture. By understanding the extent of flooding and floodwater inundation, we can decide how to best allocate resources to prepare for emergencies.*

**Keywords:** Flood; Inundation; HEC-RAS Modelling

### Introduction

Flood inundation is the most common and one of the most serious natural disaster phenomena around the world. Hazards associated with flooding can be divided into primary hazards that occur due to contact with water, secondary effects that occur because of the flooding, such as disruption of services, health impacts, famine and disease, and tertiary effects such as changes in the position. Throughout the last century flooding has been one of the costliest disasters in terms of both property damage and human casualties.

Flooding is one of the most damaging natural hazards to human societies.

Recent decades have shown that flooding constitutes major threats worldwide, and due to anticipated climate change the occurrence of damaging flood events is expected to increase. It occurs when too much water exists for the carrying capacity and infiltration rates of the soil. Areas prone to flooding are floodplains and are generally located near a waterway.

In recent decades, flooding increased profoundly largely due to hydrological characteristics changes. These floods usually occurred annually during the Monsoon from July to October. Following the population growth, it accentuates human activities such as uncontrolled development where green areas initially function as natural sponge have been paved

leading to increase in impervious areas and surface runoff.

There was considerable increase in the occurrence of floods and flood-related damage globally during 2006. The flood events accounted for nearly 55% of all disasters registered and approx. 72.5% of total economic losses worldwide. This is the reason why flooding is considered as the world’s costliest type of natural disaster in terms of both human casualties and property damage. The annual disaster review indicates that flood occurrence has increased almost 10-fold during the last 45 years, from just 20 events in 1960, to 190 events in 2005. In India, about 40 million ha of land is flood prone, which is about 12% of the total geographical area (328 million ha) of the country. The flooding occurs typically during the monsoon season (July–September), caused by the formation of heavy tropical storms, ever decreasing channel capacity due to encroachments on river beds, and sometime due to tidal backwater effects from the sea.

The HEC-RAS model is one of the most popular hydraulic models, recently used in many studies for dam break analysis, preparation flood inundation maps, flood prone area, water surface elevation map (Knebl et al). The Results of the HEC-RAS will help to identify the height of flood prevention structures in the flood prone area. The purpose of the study is preparation of flood Inundation map using HEC-RAS model and GIS with prediction of water spread, depth of water along with probable maximum flood.

### Study Area

The Tungabhadra River is formed by the confluence of two rivers, the Tunga River and the Bhadra River which originates in Varaha Parvatha in the Western Ghats and joins at Kudali village in Shimoga District at an elevation of about 610metres. It flows along the mutual boundary of Bellary and Raichur districts and joins the river Krishna near Kurnool in Andhra Pradesh. Major tributaries of the Tungabhadra River are the Bhadra, the Haridra, the Vedavati, the Tunga, the Varda, and the Kumdavathi.

The study area is a part of the Tungabhadra River extracted from the main river which is located near the discharge site Haralahalli. Haralahalli is a small Village/hamlet in Haveri Taluk in Haveri District of Karnataka State, India. It comes under Haralahalli Panchayath. It belongs to Belgaum Division. It is located 33 KM towards East from District headquarters Haveri. 21 KM from Haveri. 344 KM from State capital Bangalore the lower stream and upper stream is extracted based on tributary from the mainstream.

It flows for a distance of 293 km. in the State of Karnataka. It has a total drainage area of 47287 square kilometers. The average annual discharge of Tungabhadra at its confluence with Krishna is 14700 million m<sup>3</sup>. Tungabhadra River in total constitutes 104 watersheds, covering a total area of 70075.89 sq. km.

### STUDY AREA DELINIATION

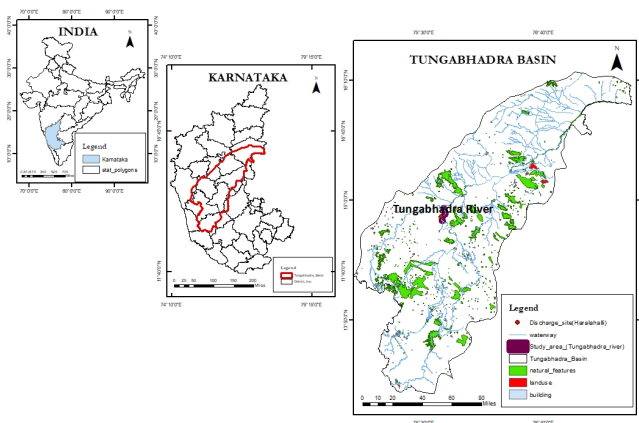


Fig. 1. Study area Delineation

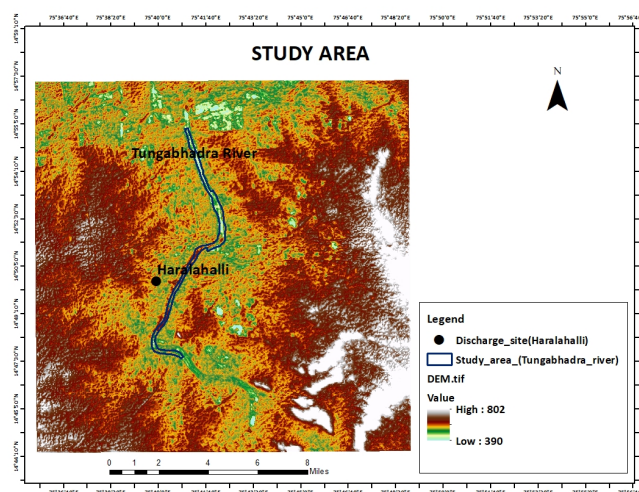


Fig. 2. Study area (part of Tungabhadra River)

### Objectives

These are the main objectives which will be persuaded to achieve the aim above.

- To create a Flood Inundation Model of Haralahalli Discharge Site in Tungabhadra Basin.
- To determine the Maximum and Minimum Inundation Boundary of the Haralahalli Discharge Site in Tungabhadra Basin.

### Methodology

The methodology/procedures followed in the project work are the process involved in determining the water surface level and depth of the inundated water, inundation boundary, and velocity of the river.

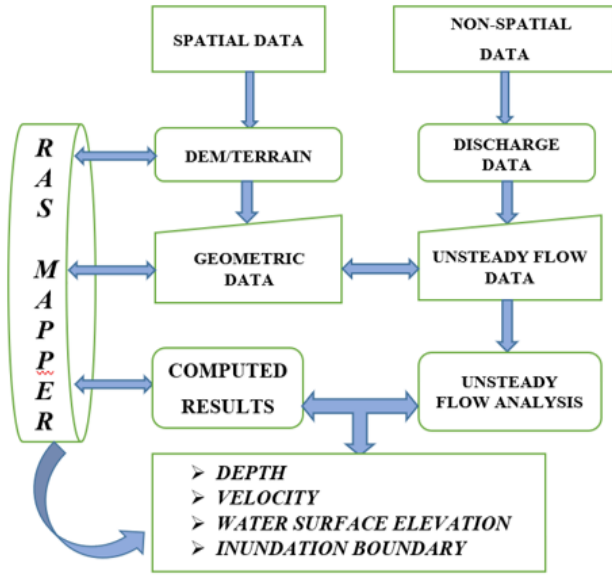


Fig. 3. Flow chart of methodology

### Methods of Data Analysis

The SRTM-DEM image downloaded from USGS Earth Explorer is used for generating Geometry for determining the river reach by digitizing the streamline, bank line, flow path, and cross-sections.

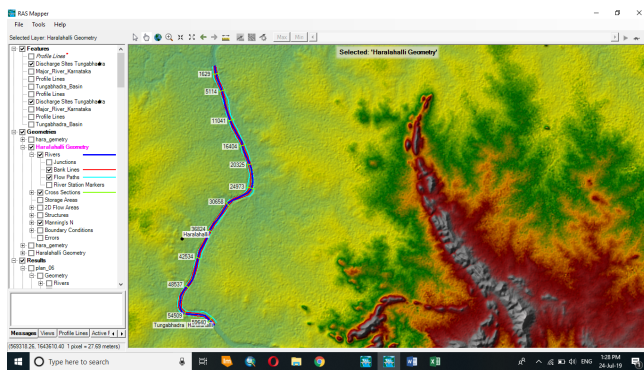


Fig. 4. Creating Geometric data in HEC-RAS

The length of the river reach considered for the analysis is 17800.82 meters and the width of the river varies in each cross-section for different years. These geometric data (River, Bank line, Flow path) is then used to perform the unsteady flow analysis with the discharge data. The first cross-section and the last cross-section determine the upstream and lower stream boundary respectively.

The manning values of the study area are given as 0.035 and 0.05 based on the geometric data (ruggedness and roughness of the terrain). And the normal depth is given as

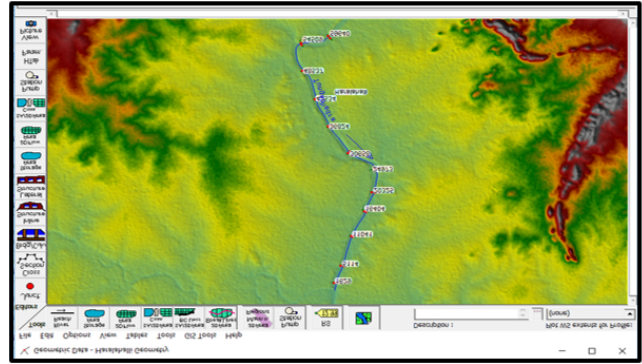


Fig. 5. Geometric Data of Tungabhadra river at Haralahalli town defining the river reach.

0.001.

River Station	Frctn (n/k)	n #1	n #2	n #3
1 59640	n	0.05	0.035	0.05
2 54509	n	0.05	0.035	0.05
3 48537	n	0.05	0.035	0.05
4 42534	n	0.05	0.035	0.05
5 36824	n	0.05	0.035	0.05
6 30658	n	0.05	0.035	0.05
7 24973	n	0.05	0.035	0.05
8 20325	n	0.05	0.035	0.05
9 16404	n	0.05	0.035	0.05
10 11041	n	0.05	0.035	0.05
11 5114	n	0.05	0.035	0.05
12 1629	n	0.05	0.035	0.05

Fig. 6. Manning's value

The discharge data is entered in the unsteady flow data as the flow hydrograph for the upstream boundary i.e. the first cross-section or river station. For the downstream boundary i.e. the last cross-section the normal depth is entered as 0.001.

Date	Simulation Time (hours)	Flow (m <sup>3</sup> /s)
01/01/2006 2400	2400	104.8
01/01/2006 2400	2400	217.2
01/01/2006 2400	4800	5097
01/01/2006 2400	7200	206.4
01/01/2006 2400	9600	5036
01/01/2006 2400	12000	1322
01/01/2006 2400	14400	1134
01/01/2006 2400	16800	1013
01/01/2006 2400	19200	803.7
01/01/2006 2400	21600	704.5
01/01/2006 2400	24000	438.2
01/01/2006 2400	26400	443.2
01/01/2006 2400	28800	119.2
01/01/2006 2400	31200	44.4
01/01/2006 2400	33600	14.5

Fig. 7. Unsteady flow data

### Discharge Data Analysis of Haralahalli Town

Keeping in mind the objective of the research of this study, the analysis was carried out. The results are presented in the



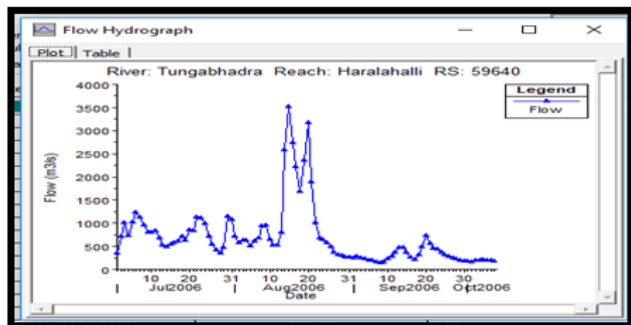


Fig. 8. Flow Hydrograph of the lower stream

form of maps, tables and histograms. They include some static change in the inundation boundary of Haralahalli Discharge Site in Tungbhadra Basin.

**Unsteady Flow Analysis**

For the entered Unsteady Flow Data analysis is performed by selecting the simulation time window i.e. from July 1st to September 30th in this case. This period of three peak monsoon months is considered because the discharge and water level is at peak level during monsoon. Considering these criteria, the analysis is performed for the three different years is 2006,2011 & 2016 respectively. The interval settings for different computations to be performed are to be given as 1 day as the discharge/flow data entered in unsteady flow data was for the same interval. Thereby, the computation results would vary for each day in the time window wherein the Maximum and Minimum values of Depth of inundation, Velocity of Flow, Water Surface Elevation, and other necessary results can be displayed.

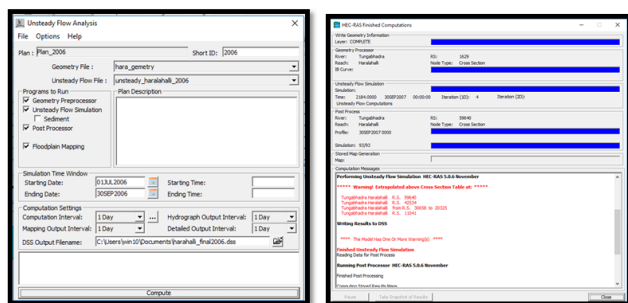


Fig. 9. Dialog box showing Unsteady flow process

The results computed by unsteady flow analysis can be visualized in the RAS Mapper.

**Depth**

The depth of the water inundated in the river reach and the right and left bank can be visualized and the value in meters

can be shown by rolling the mouse cursor over the layer.

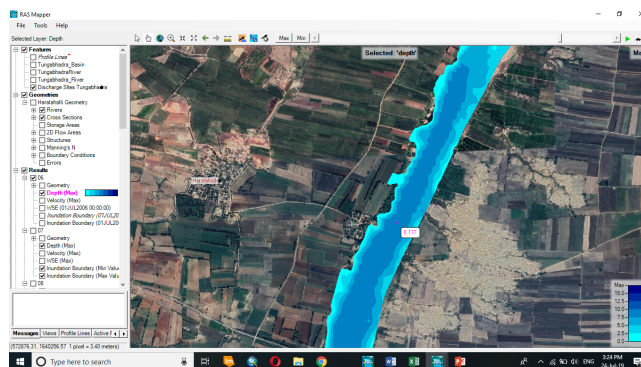


Fig. 10. Inundation model showing depth of the river

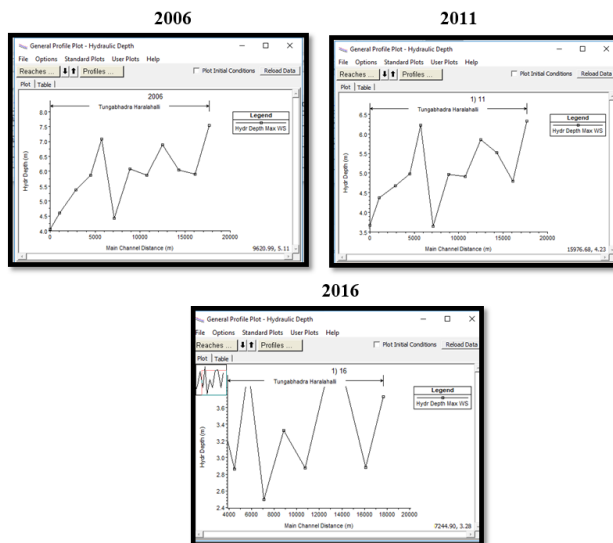


Fig. 11. Showing the depth of the river at each cross section

**Velocity**

The velocity is the rate of flow of water over a unit area per second determined in units of square meters per second (m<sup>2</sup>/sec).



Fig. 12. Inundation model showing velocity of the river



The graph plots for channel velocities are obtained from the general plot option. These plots determine the variation of the velocity along the length of the river reach.

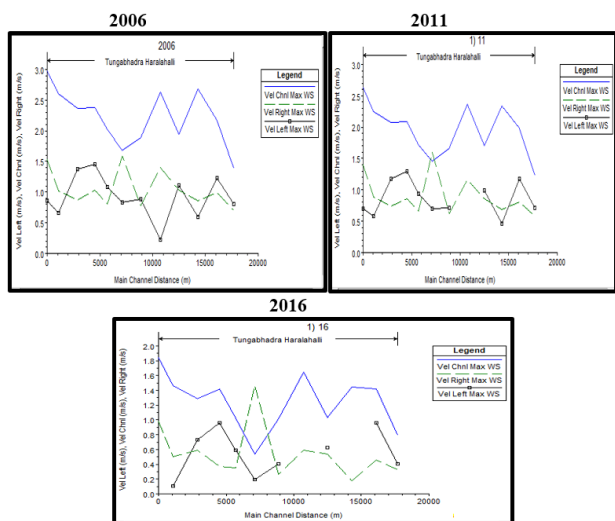


Fig. 13. Showing the velocity of the river at each cross section

### Water Surface Elevation (WSE)

The Water Surface Elevation is the elevation of water surface measured above mean sea-level. The value and variation of the Water Surface Elevation can be visualized and interpreted similarly to Depth and Velocity. The sum of Terrain value and depth value over the river reach will give the value of WSE.



Fig. 14. Inundation model Water Surface Elevation of the river

The profile plot depicts the maximum water surface level along the length of the river reach.

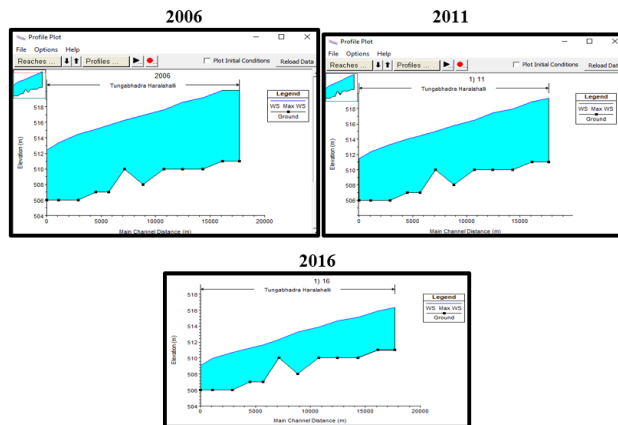


Fig. 15. Showing the maximum Water Surface Elevation

### Cross Section

The cross-section graph for the upstream (first cross-section) and the lower stream boundary (last cross-section) of the river can be analyzed. The graph shows the maximum water surface level concerning the ground level of the river bed terrain along the width of the river reach.

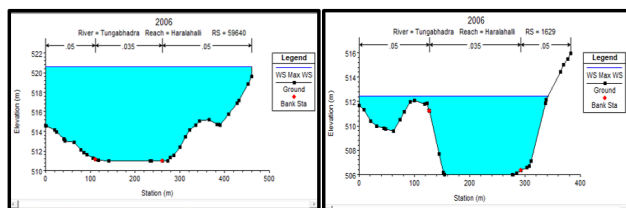


Fig. 16. Cross section plot of upper stream and lower stream boundary for the year 2006

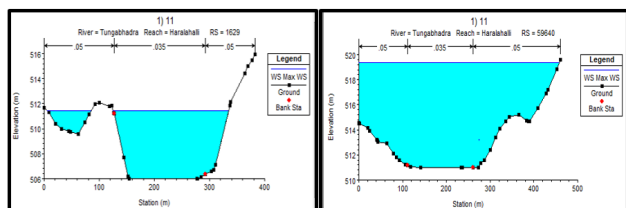


Fig. 17. Cross section plot of upper stream and lower stream boundary for the year 2011

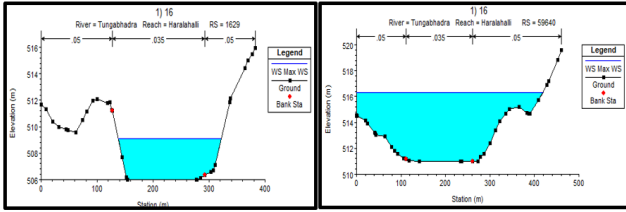


Fig. 18. Cross section plot of upper stream and lower stream boundary for the year 2016

**Cross Section Output**

The cross-section table can be obtained for each cross-section for the outputs of different unsteady flow data.

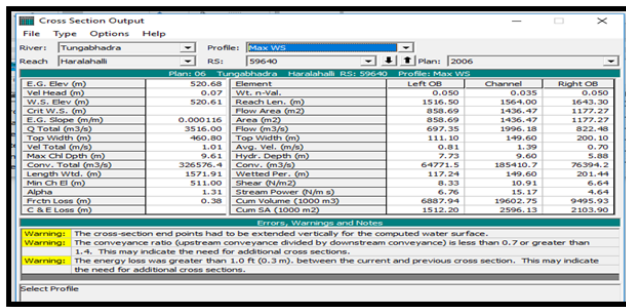


Fig. 19. Cross section output

This output shows the values of different variables such as discharge(Q), Top width, W.S Elevation, Channel Elevation, Velocity, etc. which may facilitate various interpretations. The cross-section table can be obtained for each cross-section for the outputs of different unsteady flow data.

**XYZ Perspective plot**

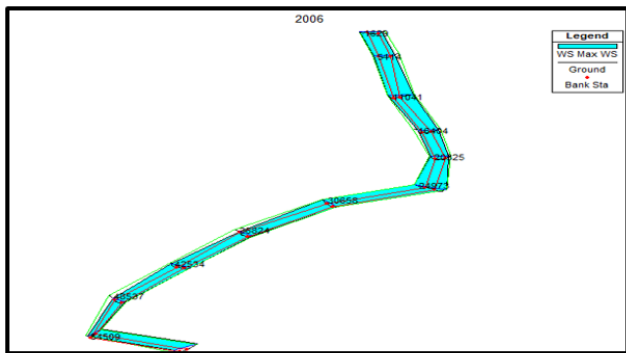


Fig. 20. 3-D View of the river geometry

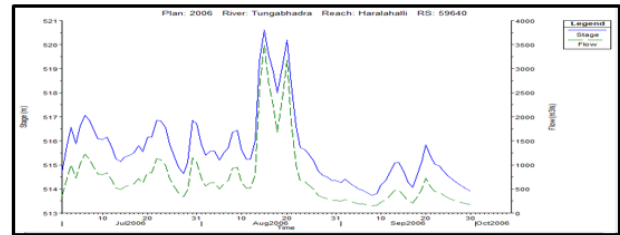
This plot represents the river reach geometry concerning Maximum water surface level in an XYZ i.e. a 3-dimensional perspective. The plot can be visualized from different angles

for better interpretation.

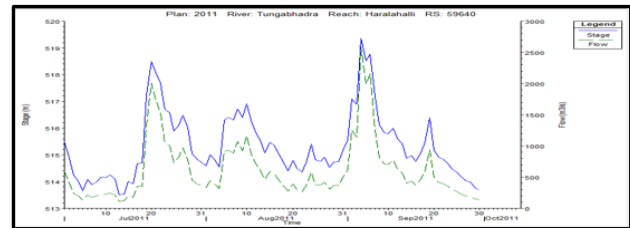
**Results and Discussion**

We can see that the maximum and the minimum water surface elevation for the year 2006 is the highest in 2006 and the lowest in 2016. Subsequently, the result shows a decrease in the volume of water flowing at each cross-section in 2006, 2011, 2016. The depth of the water is also decreasing, in 2006 the average depth was approximately 9 meters, and in 2011 it decreased to 7 meters, and similarly, in 2016 it went down to 4 meters. It can also be seen on the map that the maximum and minimum inundated boundary is varying. Since the ground elevation (river bed) of the area is approximately 10 meters less than the ground elevation of the area.

2006



2011



2016

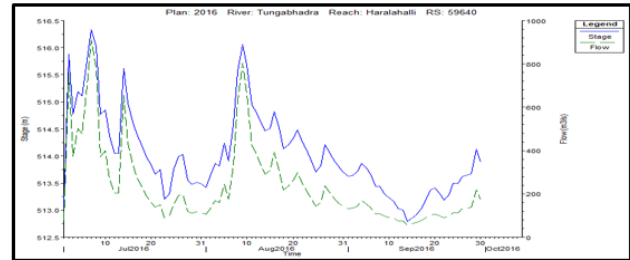


Fig. 21. Discharge and the stage data

The depth of the river is decreasing consequently, as seen in this study. The reason for this can be the sedimentation or the depositional activities happening under the river. Another reason can be the discharge of the water that is flow, it can be seen in the table below that the flow has also a decrease in its level.

So, from this study, it is seen that the river is under the deprivation of water. The width of the river, it's surface water



elevation, its depth is decreasing. The study area falls in the middle of the basin where the terrain is mostly plain with minimum rainfall so it can be recommended to induce rainwater harvesting and building of dams to store water.

Though there is no increase in the water surface elevation or the depth of the river in the last 10 years, if in the future the discharge level reaches its peak, maybe 20times more than it is seen now, then there will be an obvious chance of flood in the floodplain area. So, this study can be used for future reference purposes. Below are the graphs showing the discharge and the stage data of the Haralahalli site for upper stream and lower stream for the year 2006, 2011, and 2016

The maps below show the maximum and the minimum Inundation boundary of the Tungabhadra river for the years 2006, 2011, and 2016. The minimum Inundated boundary is highest for the year 2006 and lowest for the year 2016, which clearly says that there is no flood in the floodplains and nearby areas

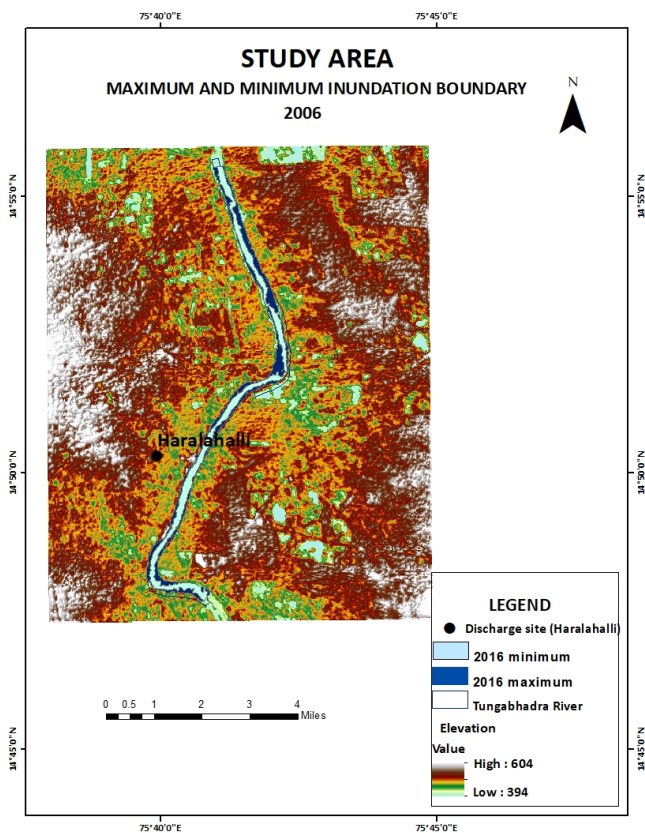


Fig. 22. Maximum and Minimum Inundation map of the year 2006

The changes can be seen and compare among the three years 2006, 2011, 2016. It can be seen in Discharge level, velocity, and depth at each cross-section of the river

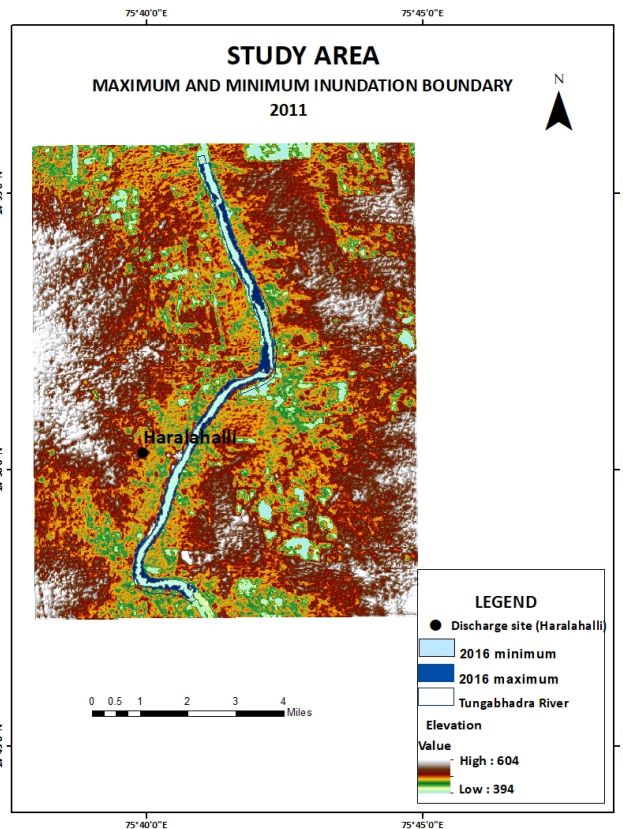


Fig. 23. Maximum and Minimum Inundation map of the year 2011

### Conclusion

This paper presents a methodology for developing a flood model for the Haralahalli Discharge site, Tungabhadra river. The hydraulic modeling with GIS integration makes the modeling process easy and produces more easily understandable results. In this study, a part of the Tungabhadra main river was taken as the study area at the Haralahalli discharge site. The study area consists of a few locations where the floodplain area is utilized for farming while the other consists of residential areas. To sum up of the current work is that the HEC-RAS (one-dimensional model) can be used successfully to get the maximum and the minimum water inundation boundary. Also, GIS is the viable software to generate the maps of water inundated areas as estimated by HEC-RAS for different peak outflow scenarios. It is, therefore, necessary to make proper plans to reduce the risk associated with flooding events in the country. Remote sensing technique integrated with GIS has proved to be the most effective way of identifying and mapping the flood inundated areas. There is an immense need to apply remote sensing and GIS methods to map the flood vulnerable areas in the region by using more advanced available techniques. There is a great potential in the current field of research encompassing various hydrological and climatolog-



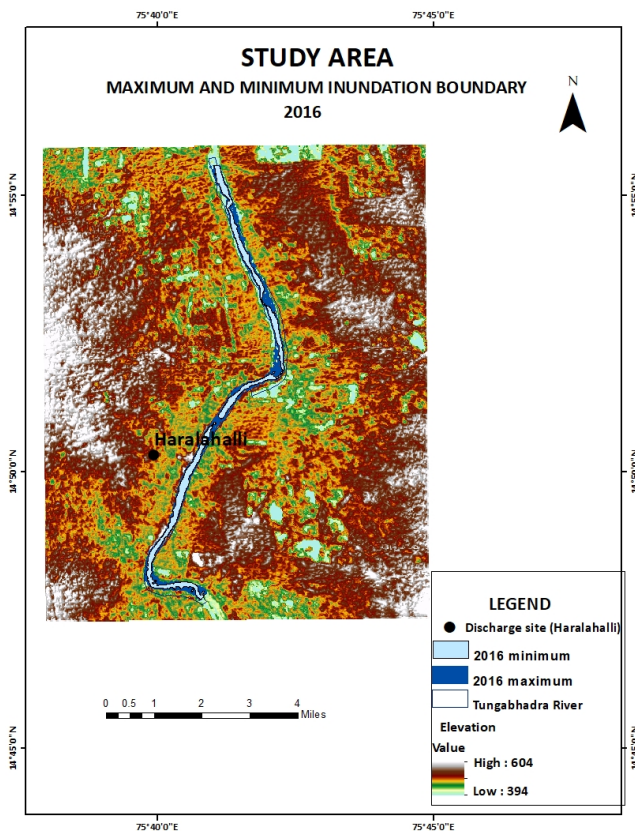


Fig. 24. Maximum and Minimum Inundation map of the year 2016

2006												
Reach	River Sta	Profile	Q Total (m <sup>3</sup> /s)	Min Ch El (m)	W.S. Elev (m)	Crit W.S. (m)	E.G. Elev (m)	E.G. Slope (m/m)	Vel Chnl (m/s)	Flow Area (m <sup>2</sup> )	Top Width (m)	Froude # Chl
Haralshali	59640	Max WS	3516.00	511.00	520.61		520.68	0.000116	1.39	3472.43	460.80	0.14
Haralshali	54509	Max WS	3906.38	511.00	520.13		520.32	0.000369	2.17	2144.73	362.84	0.25
Haralshali	48537	Max WS	3498.38	510.00	519.16		519.51	0.000539	2.68	1435.26	237.57	0.20
Haralshali	42534	Max WS	3490.60	510.00	518.61		518.75	0.000263	1.95	2431.58	353.25	0.21
Haralshali	36824	Max WS	3483.05	510.00	517.65		517.96	0.000670	2.63	1523.90	259.69	0.32
Haralshali	30658	Max WS	3474.60	508.00	516.90		517.05	0.000251	1.89	2395.52	394.50	0.21
Haralshali	24973	Max WS	3462.98	510.01	516.25		516.37	0.000509	1.68	2376.50	536.35	0.26
Haralshali	20325	Max WS	3454.52	507.00	515.64		515.82	0.000284	2.02	2024.08	286.05	0.22
Haralshali	16404	Max WS	3449.30	507.00	515.14		515.37	0.000475	2.38	1819.70	309.85	0.28
Haralshali	11041	Max WS	3441.25	506.00	514.46		514.66	0.000399	2.37	2119.54	394.58	0.26
Haralshali	5114	Max WS	3432.43	506.00	513.39		513.71	0.000651	2.61	1528.95	333.03	0.32
Haralshali	1629	Max WS	3427.82	506.00	512.45		512.85	0.000999	2.98	1386.94	341.90	0.39

2011												
Reach	River Sta	Profile	Q Total (m <sup>3</sup> /s)	Min Ch El (m)	W.S. Elev (m)	Crit W.S. (m)	E.G. Elev (m)	E.G. Slope (m/m)	Vel Chnl (m/s)	Flow Area (m <sup>2</sup> )	Top Width (m)	Froude # Chl
Haralshali	59640	Max WS	2593.00	511.00	519.36		519.42	0.000110	1.23	2897.84	458.18	0.14
Haralshali	54509	Max WS	2574.93	511.00	518.89		519.05	0.000389	1.99	1698.65	353.77	0.25
Haralshali	48537	Max WS	2560.76	510.00	517.97		518.24	0.000505	2.33	1168.43	211.50	0.28
Haralshali	42534	Max WS	2547.38	510.00	517.43		517.54	0.000245	1.70	2018.74	345.23	0.20
Haralshali	36824	Max WS	2534.39	510.00	516.51		516.77	0.000667	2.37	1233.54	251.09	0.31
Haralshali	30658	Max WS	2520.36	508.00	515.78		515.90	0.000237	1.67	1951.15	392.38	0.20
Haralshali	24973	Max WS	2501.90	510.01	515.06		515.17	0.000595	1.45	1763.24	483.84	0.27
Haralshali	20325	Max WS	2488.58	507.00	514.44		514.57	0.000249	1.71	1691.15	271.60	0.30
Haralshali	16404	Max WS	2480.12	507.00	513.98		514.16	0.000456	2.09	1468.62	294.79	0.26
Haralshali	11041	Max WS	2467.21	506.00	513.33		513.49	0.000372	2.08	1692.58	362.16	0.25
Haralshali	5114	Max WS	2453.96	506.00	512.36		512.60	0.000604	2.25	1213.73	278.00	0.30
Haralshali	1629	Max WS	2447.45	506.00	511.44		508.99	0.001000	2.64	1063.89	282.83	0.38

2016												
Reach	River Sta	Profile	Q Total (m <sup>3</sup> /s)	Min Ch El (m)	W.S. Elev (m)	Crit W.S. (m)	E.G. Elev (m)	E.G. Slope (m/m)	Vel Chnl (m/s)	Flow Area (m <sup>2</sup> )	Top Width (m)	Froude # Chl
Haralshali	59640	Max WS	911.60	511.00	516.33		516.36	0.000082	0.79	1565.19	419.16	0.11
Haralshali	54509	Max WS	908.04	511.00	515.87		515.96	0.000449	1.42	751.19	261.00	0.24
Haralshali	48537	Max WS	905.43	510.00	515.08		515.19	0.000392	1.45	628.60	161.91	0.23
Haralshali	42534	Max WS	902.60	510.00	514.63		514.67	0.000168	1.03	1129.41	292.74	0.15
Haralshali	36824	Max WS	899.62	510.00	513.88		514.01	0.000611	1.65	600.62	208.93	0.28
Haralshali	30658	Max WS	896.16	508.00	513.23		513.28	0.000153	1.02	1043.93	313.95	0.15
Haralshali	24973	Max WS	892.57	510.01	512.31		512.41	0.000848	0.54	645.91	258.95	0.24
Haralshali	20325	Max WS	890.19	507.00	511.65		511.70	0.000165	1.02	978.97	239.29	0.15
Haralshali	16404	Max WS	888.30	507.00	511.25		511.34	0.000446	1.42	718.17	251.26	0.24
Haralshali	11041	Max WS	885.80	506.00	510.70		510.76	0.000259	1.28	874.30	230.85	0.19
Haralshali	5114	Max WS	883.44	506.00	509.95		510.05	0.000525	1.46	626.26	209.19	0.26
Haralshali	1629	Max WS	882.32	506.00	509.08		507.57	0.001002	1.84	506.38	183.97	0.34

Fig. 25. Showing the discharge, velocity and water surface elevation

ical application scenarios. It is envisaged that further work in the current field will help us to better understand the flow and inundation and its consequent results for the policymakers and planners. The resulting flood inundation maps are useful for municipal planning purposes, emergency action plans, flood insurance rates, and ecological studies. So, it can be concluded that though there is no increase in water level but future floods may occur, and this model can be proved handy for real-time flood mapping in case of emergency and immediate relief measures can be adopted accordingly if in case any future flood occurs in the river.

References

- Safaripour, M., Monavari, M., Zare, M., Abedi, Z., & Gharagozlou, A. (2012). Flood Risk Assessment Using GIS (Case Study: Golestan Province, Iran). Polish Journal of Environmental Studies.
- Youssef, Ahmed M., Biswajeet Pradhan, and Abdallah Mohamed Hassan. "Flash flood risk estimation along the St. Katherine road, southern Sinai, Egypt using GIS based morphometry
- Sowmya, K., C. M. John, and N. K. Shrivasthava. "Urban flood vulnerability zoning of Cochin City,

southwest coast of India, using remote sensing and GIS"

- Singh, Anupam K., and Arun K. Sharma. "GIS and a remote sensing-based approach for urban floodplain mapping for the Tapi catchment, India." IAHS publication 331 (2009): 389.
- Wicht, Marzena, and Katarzyna Osinska-Skotak. "Identifying urban areas prone to flash floods using GIS—preliminary results."
- Khattak, Muhammad Shahzad, et al. "Floodplain mapping using HEC-RAS and ArcGIS: a case study of Kabul River." Arabian Journal for Science and Engineering 41.4 (2016): 1375-1390.
- Rangari, Vinay Ashok, et al. "Floodplain Mapping and Management of Urban Catchment Using HEC-RAS: A Case Study of Hyderabad City."
- Goodell, C., and C. Warren. "Flood inundation mapping using HEC-RAS." Obras y Proyectos (2006):
- Kowalczyk, Zdzisław, Mateusz Świergal, and Mirosław Wróblewski. "River flow simulation based on the HEC-RAS system." International Conference on Diagnostics of Processes and Systems. Springer, Cham, 2017.



10. Surwase, Tushar, et al. "Flood Inundation Simulation of Mahanadi River, Odisha During September 2008 by Using HEC-RAS 2D Model." Proceedings of International Conference on Remote Sensing for Disaster Management. Springer, Cham, 2019.
11. Kumar, Neeraj, et al. "Applicability of HEC-RAS & GFMS tool for 1D water surface elevation/flood modeling of the river: a Case Study of River Yamuna at Allahabad (Sangam), India." Modeling Earth Systems and Environment 3.4 (2017): 1463-1475.
12. Panda, Prafulla Kumar, and Santiswarup Sahoo. "Modelling of Floodplain Using Recent Technology." European Journal of Advances in Engineering and Technology 2.7 (2015): 23-28.
13. Das, Bahnisikha, and B. S. Sil. "Assessment of Sedimentation in Barak River Reach Using HEC-RAS." Development of Water Resources in India. Springer, Cham, 2017. 95-102.
14. Hammond, Michael J., et al. "Urban flood impact assessment: A state-of-the-art review." Urban Water Journal 12.1 (2015): 14-29.